Default mode network activity in schizophrenia studied at resting state using probabilistic ICA

Gianluca Mingoia [a,*], Gerd Wagner [a], Kerstin Langbein [a], Raka Maitra [a], Stefan Smesny [a], Maren Dietzek [a], Hartmut P. Burmeister [b], Jürgen R. Reichenbach [c], Ralf G.M. Schlösser [a], Christian Gaser [a], Heinrich Sauer [a], Igor Nenadic [a,**]

[a] Department of Psychiatry and Psychotherapy, Jena University Hospital, Jena, Germany
[b] Institute for Diagnostic and Interventional Radiology I (IDIR I), Jena University Hospital, Jena, Germany
[c] Medical Physics Group, Institute for Diagnostic and Interventional Radiology I (IDIR I), Jena University Hospital, Jena, Germany

ARTICLE INFO

ABSTRACT

Alterations in brain function in schizophrenia and other neuropsychiatric disorders are evident not only during specific cognitive challenges, but also from functional MRI data obtained during a resting state. Here we apply probabilistic independent component analysis (pICA) to resting state fMRI series in 25 schizophrenia patients and 25 matched healthy controls. We use an automated algorithm to extract the ICA component representing the default mode network (DMN) as defined by a DMN-specific set of 14 brain regions, resulting in z-scores for each voxel of the (whole-brain) statistical map. While goodness of fit was found to be similar between the groups, the region of interest (ROI) as well as voxel-wise analysis of the DMN showed significant differences between groups. Healthy controls revealed stronger effects of pICA-derived connectivity measures in right and left dorsolateral prefrontal cortices, bilateral medial frontal cortex, left precuneus and left posterior lateral parietal cortex, while stronger effects in schizophrenia patients were found in the right amygdala, left orbitofrontal cortex, right anterior cingulate and bilateral inferior temporal cortices. In patients, we also found an inverse correlation of negative symptoms with right anterior prefrontal cortex activity at rest and negative symptoms. These findings suggest that aberrant default mode network connectivity contributes to regional functional pathology in schizophrenia and bears significance for core symptoms.

1. Introduction

Functional magnetic resonance imaging (fMRI) has mostly been used to assess deficits of task-induced activation, e.g. during working memory tasks (Minzenberg et al., 2009). More recent studies have provided evidence for alterations detectable already under "resting state" conditions, i.e. without performing a specific cognitive task. While such resting-state abnormalities have been observed in several neuropsychiatric disorders (Greicius, 2008; Broyd et al., 2009), these findings bear particular significance for schizophrenia, as they might be related to cognitive impairment and clinical symptoms.

The approaches to analyse resting-state fMRI data in schizophrenia all exploit the fact that the BOLD signal shows low-frequency fluctuations (Auer, 2008), which are assumed to be linked to resting-state networks (Damoiseaux et al., 2006). While some studies have demonstrated changes on regional amplitude of low-frequency fluctuations during rest (Huang et al., 2009; Hoptman et al., 2010), others have used either correlation of seed-regions such as the posterior cingulate cortex (PCC) with other brain areas (Bluhm et al., 2007), or have used independent component analysis (ICA) to extract sets of regions following a similar time course (Garrity et al., 2007). Despite different methodologies, these studies appear to overlap in alteration of nodes of the default mode network (DMN), esp. the medial prefrontal cortex.

The default mode network (DMN) is a concept based on an interconnected set of areas showing higher activity during rest than task-related activity (Raichle et al., 2001; Raichle and Snyder, 2007). This network has been defined by initial studies of Shulman et al. based on changes of cerebral blood flow during visual tasks (Shulman et al., 1997). Since then it has been studied extensively with both seed-ROI based correlations and ICA methods (Raichle and Snyder, 2007; van den Heuvel and Hulshoff Pol, 2010), and linked to electrophysiological activity in the beta and gamma band (Mantini et al., 2007).

Recent studies on DMN activity in schizophrenia have suggested medial prefrontal cortical areas of the DMN network to show aberrant connectivity or activity, although the evidence is not completely converging on this area and direction of effects differ across studies (Zhou et al., 2007; Kim et al., 2009; Whitfield-Gabrieli et al., 2009; Ongur et al.,

2010; Woodward et al., 2011). However, these studies show links to both cognitive deficits and to symptoms (Rotarska-Jagiela et al., 2010), which links them to the relevant pathophysiology of schizophrenia. Moreover, other findings suggest a relative specificity of certain abnormalities for schizophrenia (Calhoun et al., 2008).

In the present study, we aimed to analyse resting state data, devoid of any directed cognitive task, using probabilistic independent component analysis (pICA) in a cohort of chronic schizophrenia patients in order to test the hypothesis of activity differences across the nodes of the DMN. More specifically, we aimed to test that prefrontal differences in resting state DMN activity are evident in resting-state conditions in the absence of cognitive stimulation, and in patients with remission of psychotic episode. We applied an algorithm using an overall approach similar to Greicius (Greicius et al., 2004, 2007), focussing on an automated detection/extraction of the DMN component and group comparison, in order to eliminate the necessity for observer-dependent interventions such as placement of seed regions. We tested the hypothesis of impaired frontal cortical connectivity by studying remitted patients, i.e. not during a psychotic episode, and correlated data with negative symptoms.

2. Methods

2.1. Study participants

We studied 25 patients with DSM-IV schizophrenia (8 female; mean age 30 years, SD 7.3; age range 21–49 years) and 25 healthy controls (10 female; mean age 29.1 years, SD 8.6; age range 22–55 years), of which three patients were left-handed as determined by the Edinburgh Handedness Scale (Oldfield, 1971). Proportion of left-handers did not differ between groups (Fisher Exact Probability Test p > 0.23). All participants gave written informed consent to participation in this study, which was conducted as part of the EUTwinsS project (European Twin Study Network on Schizophrenia) and approved by the Ethics Committee of the Friedrich-Schiller-University Medical School, Jena. None of the participants had a neurological condition of history of traumatic brain injury or learning disability. We carefully interviewed all participants to exclude candidates with a present or previous neurological CNS condition, history of traumatic brain injury, or learning disability. In addition, patient records were reviewed, where available, to ensure patients did not meet any of these exclusion criteria. According to chart review, none of the patients had a concurrent axis II disorder. In addition, all participants were screened using the MWT-B, a standardised and widely-used German test assessing (pre-morbid) IQ, to ensure that none of the participants had an IQ below 80.

Patients were recruited from the in-patient and out-patient services of the Department of Psychiatry and Psychotherapy in Jena. All patients had a diagnosis of schizophrenia established using DSM-IV criteria (American Psychiatric Association). A board-certified psychiatrist (I.N.) assessed each patient, conducting an additional chart review where necessary, and also rated current psychopathology using the Scale for Assessment of Negative Symptoms (SANS), the Scale for Assessment of Positive Symptoms (SAPS), and the Brief Psychiatric Rating Scale (BPRS). All patients were remitted, i.e. none of them was experiencing an acute psychotic episode at the time of the study, and hence they showed mostly residual negative psychopathology and only little positive symptoms.

Healthy control subjects were recruited from the local community and matched to the patients with regard to age, gender, and handedness (details of demographics and comparison are given in Table 1; T-Test for age difference: p > 0.66, two-tailed; Chi-square test for gender: p > 0.53; Fisher Exact Test for handedness: P > 0.11, one-tailed). They underwent a semi-structured interview to exclude personal history or any current psychiatric disorder.

Table 1
Demographical data of subject samples.

	Patients	Controls
Number	25	25
Gender	8 females, 17 males	10 females, 15 males
Age (mean ± SD)	30 ± 7.3 years	29.1 ± 8.6 years
SANS total score (mean ± SD)	40.3 (14.5)	N/A
SAPS total score (mean ± SD)	21.8 (11.7)	N/A
BPRS total score (mean ± SD)	38.9 (7.3)	N/A

2.2. Data acquisition and pre-processing

We obtained resting-state fMRI series on a 3 T Siemens Tim Trio system (Siemens, Erlangen, Germany) using the 12-channel head matrix coil. Subjects were instructed to relax and keep their eyes closed (without falling asleep, which was confirmed immediately after the scanning session). Foam pads were used for positioning and immobilisation of subjects' heads during scanning. We obtained a series of 210 T2*-weighted whole-brain volumes over approx. 9 min, using a standard BOLD-sensitive EPI sequence (TR 2550 ms; TE 30 ms; flip angle 90°; 45 contiguous axial slices with 3 mm thickness, no gap, matrix 64×64; in-plane resolution of 3×3 mm; field-of-view 192 mm × 192 mm). In addition, we acquired a high-resolution structural scan for co-registration using a 3D MPRAGE sequence with 192 contiguous sagittal slices of 1 mm thickness (TR 2300 ms; TE 3 ms; TI 900 ms; echo time 8.9 ms; flip angle 9°; matrix size 256×256; isotropic voxel dimensions of 1×1×1 mm).

Both functional and structural images series underwent a quality assurance protocol, including visual inspection, and none of the participants showed such artefacts.

Data analysis was performed using SPM5 (Institute of Neurology, London, UK; www.fil.ion.ucl.ac.uk/spm) for pre-processing as well as later voxel-wise statistics, and FSL MELODIC for independent component analysis (FMRIB, University of Oxford, UK; www.fmrib.ox.ac.uk/fsl/melodic2/index.html).

We first discarded the first three images of each functional series to avoid T1 saturation effects. In order to remove movement artefact, images were realigned using a least-squares approach and a 6-parameter rigid body spatial transformation. A two-pass procedure was used to register the images to the mean of the images after the first realignment. We applied smoothing with a 4 mm FWHM Gaussian kernel before estimating the realignment parameters. None of the participants exceeded the pre-defined movement limits (3 mm translation on x, y, or z axis or 3° rotation), which were also part of the quality assurance protocol.

Within-subject registration was performed between functional images (used as reference image) and the anatomical image. Then, the co-registered anatomical images was segmented using tissue probability maps of the ICBM template (International Consortium for Brain Mapping; based on T1 scans of 452 subjects; http://www.loni.ucla.edu/ICBM/ ICBM_TissueProb.html), which were aligned with an atlas space, corrected for scan inhomogeneities, and classified into grey matter, white matter, and CSF. These data were then registered with affine transformation to MNI space and down-sampled to 2 mm resolution.

Functional images were then spatially normalised to Talairach and Tournoux space using spatial normalisation parameters estimated in the segmentation process. Images were re-sampled to 2 mm using sinc interpolation, and then smoothed with an 8 mm FWHM Gaussian kernel to account for residual inter-subject anatomical differences.

2.3. Probabilistic ICA and automated extraction of DMN component

We applied independent component analysis (ICA) using FSL software. For each subject, pre-processed functional images were

concatenated across time in a single 4D image. The MELODIC algorithm of FSL applied uses probabilistic ICA and is suited to automatically estimate the number of relevant noise and signal sources in the data. Due to this "noise model" it is possible to assign a significance value (p value) to the output spatial maps (Beckmann and Smith, 2004). The data is decomposed into a set of spatially independent maps, each with an internally consistent temporal dynamic characterised by a time course (McKeown et al., 1998). Probabilistic ICA (pICA) provides intensity values (z scores) and thus a measure of the contribution of the time course of a component to the signal in a given voxel. The individual spatial maps are therefore not mere correlations between the time course in a given voxel and the (selected) independent component, but rather the result of a multiple regression model. MELODIC therefore allows not only segregation of functional networks but also a voxel-wise map of quantitative measures of functional connectivity.

We analysed each subject's 4D image using the "FSL single-session ICA" model in MELODIC. We first applied to the time series a high-pass filter (f > 0.009 Hz) to remove low frequency drifts which can significantly contribute to the overall variance of an individual voxel's time course (Beckmann and Smith, 2004), and a low-pass filter (f < 0.18 Hz) to remove cardiac and breathing artefacts. We chose to set the ICA analysis to deliver 30 components, based on the fact that this approximates one seventh of the number of time-points in the scans.

The presence of various artefacts as Nyquist ghosting, head motion and large blood vessels strongly impacts on standard GLM analysis, which could induce additional error variance (e.g. in the case of movement-related artefacts) or show false positives (e.g. in the case of susceptibility-related artefact). Based on the Laplace approximation of the Bayesian model evidence, the pICA approach estimates components, including artefacts. The implemented MELODIC algorithm can then pick out different activation and artefactual components without any explicit time series model being specified (Beckmann and Smith, 2005). Hence, the pICA approach makes it feasible to separate uninteresting physiological noise from other effects such as resting-state maps even in cases where the physiological noise fluctuations become aliased in the temporal domain (Beckmann et al., 2005). The components relating to artefacts were removed and only the artefact not related components was included for further analysis.

We then used an automated algorithm to select the component reflecting the DMN best. For this purpose, we used a modification of the protocol devised by Greicius and colleagues applied in previous studies (Greicius et al., 2004, 2007, 2008). This was done using an in-house script developed in MATLAB. First, we anatomically defined the DMN based on the initial studies of Shulman and colleagues and subsequent studies by Raichle et al., including 14 brain areas for which we created a template defining 6 mm-diameter spheres to the centroids of each area (Shulman et al., 1997; Raichle et al., 2001). We then applied this mask image to all components (spatial maps) from the pICA analysis and masked the images with an inverse template of the DMN. We then extracted the mean z score of the masked ICA components and computed the difference between the average z score of voxels falling within the DMN template mask minus the average z score of voxels outside the template. The ICA component with the highest difference was then selected as reflecting the individual subject's DMN component. The advantage of this algorithm is that the ICA component, which corresponds to the DMN, is selected automatically, and that the computed difference score also provides an index of goodness of fit. Hence, this analysis serves to select and validate one ICA component, for which we can assume that it reflects the DMN component of the resting state signal fluctuations based on the anatomical definition of ROIs; yet, p values are given in each voxel of the (whole-brain) statistical map of this component (not only the DMN template mask).

2.4. Group statistical analyses

First, and preceding the main analyses, we compared the index of goodness of fit between the two groups. This was aimed to assess whether there is a systematic difference in the selection of the DMN component, by which the variation in goodness of fit might indicate fundamental differences of the DMN between the two groups. Group differences in goodness-of-fit would have implications for both the DMN group comparison itself and the overall integrity of the DMN.

Also, in order to assess the DMN in each group, we performed a voxel-wise random effects analysis using a one-sample *t*-test (p < 0.05 FDR corrected) in SPM, separately for each group. This was done to demonstrate the configuration and extent of the DMN component derived from pICA for patients and controls separately.

Second and third, our main analyses were the group comparison of the DMN component with an ROI-based and voxel-wise comparison, respectively. For this purpose, we first pooled the pICA-derived DMN component for all subjects into a second level analysis at p < 0.05 (uncorrected), and used the resulting statistical map as an inclusive mask to limit subsequent comparisons to those areas/voxels, which could be assumed to be significantly involved in DMN activity (based on the total cohort of subjects). We then performed an ROI analysis based on the 14 pre-defined regions derived from previous studies of the DMN (Shulman et al., 1997; Raichle et al., 2001). pICA-derived values were averaged across the voxels of each ROI and compared using SPSS 18 applying Bonferroni correction for 14 comparisons. Subsequently, we then performed a voxel-wise comparison of the two diagnostic groups in SPM using a two-sample *t*-test (p < 0.05, FDR corrected).

Finally, we performed a correlation analysis to test associations of altered DMN activity with psychopathology. For this, we focussed on the negative symptoms, which were prevalent across the patient sample, given that our patients showed rather low levels of positive symptoms (not being in a psychotic episode). We performed correlations of SANS total scores with DMN activity, restricting the analysis to ROI and voxel-wise analyses for those areas that showed differences in the above group comparisons. For this purpose, we extracted r values in individual pICA-derived DMN components of patients, averaged across the cluster and then correlated values to SANS total score using bivariate correlation analysis (Spearman's rho, implemented in SPSS 18), thresholded at p < 0.05 with FDR correction, using a MATLAB script (www.sph.umich.edu/~nichols/FDR/).

3. Results

3.1. Comparison of goodness of fit for DMN component

In all subjects, we found a component with spatial features consistent with the DMN template provided in the literature (Shulman et al., 1997; Raichle and Snyder, 2007). Comparison of goodness of fit index (as described above) between patients and controls did not show significant differences (*t*-test, one tailed: p = 0.293). The distribution of the individual scores for goodness of fit to standard default-mode network is shown in Supplementary Material 1. The voxel-wise analysis of the DMN component for each group separately is shown in Supplementary Material 2.

3.2. ROI-based and voxel-wise group comparison of DMN activity

Region of interest analysis showed significant differences in the anatomical resting state connectivity pattern of areas (Fig. 1) with healthy controls showing larger effects in the network's prefrontal and temporal areas, including the left middle frontal gyrus (BA8; close to the superior frontal junction), bilateral medial frontal gyri (BA9), bilateral superior frontal gyri (BA6), left ACC (BA32) and superior temporal sulcus (BA21/22). We found larger effects for schizophrenia patients in the right
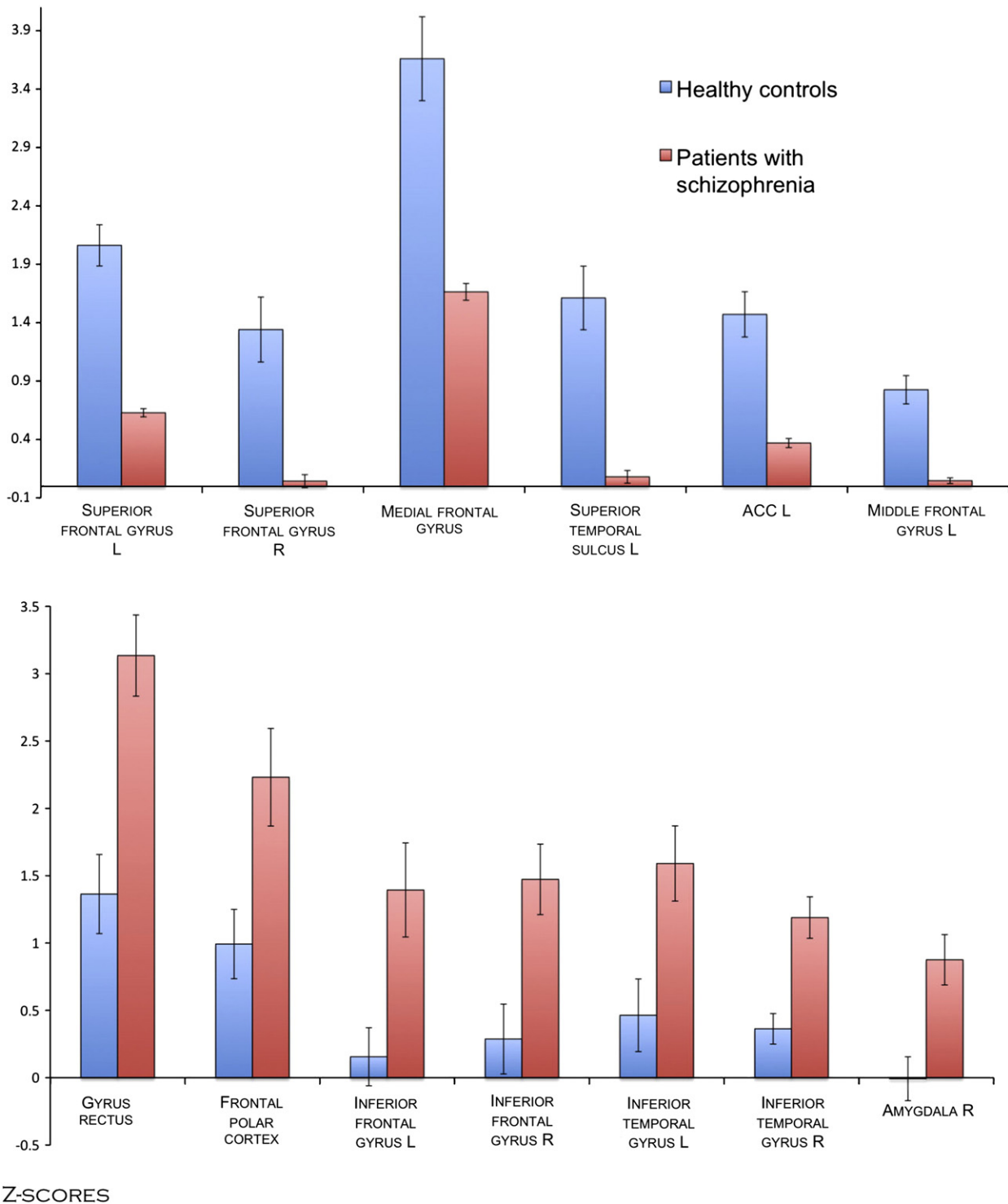
Fig. 1. ROI-based group comparison of schizophrenia patients vs. healthy control subjects of the DMN nodes; ROIs with higher z scores in healthy controls in the upper panel, those with higher z scores in schizophrenia patients in the lower panels (co-ordinates are given in Table 2A).

amygdala, middle frontal polar cortex (BA10), left gyrus rectus (BA11), bilateral inferior frontal gyri (BA47) and finally the bilateral inferior temporal gyri (BA 20). The results of the ROI based analysis (including the co-ordinates of the centroid of each area) are summarised in Table 2A.

In the voxel-wise analyses, we found significant increases in functional connectivity in controls vs. patients in a big cluster including bilateral medial frontal gyri (BA9; MNI: 5, 47, 30), left superior frontal gyrus (BA6; MNI: −9, 27, 62) and left superior temporal gyrus (BA 21/22, MNI: −53, −28, −4), and in patients vs. controls in the

middle portion of the gyrus rectus (BA11; MNI: −9, 35, −17) and the frontal polar cortex (BA10; MNI: −4, 72, −4). Results of the voxel-wise analysis are summarised in Table 2B and cortical areas are shown in Figs. 2 and 3, respectively.

3.3. Correlation of DMN and psychopathology

We restricted testing for correlations with psychopathology to those areas where patients had stronger DMN activity effects than

Table 2
Group comparison of default mode network (DMN) activity at rest for A) region-of-interest (ROI) and B) voxel-wise analyses. Co-ordinates indicate the cluster centroid in MNI space.
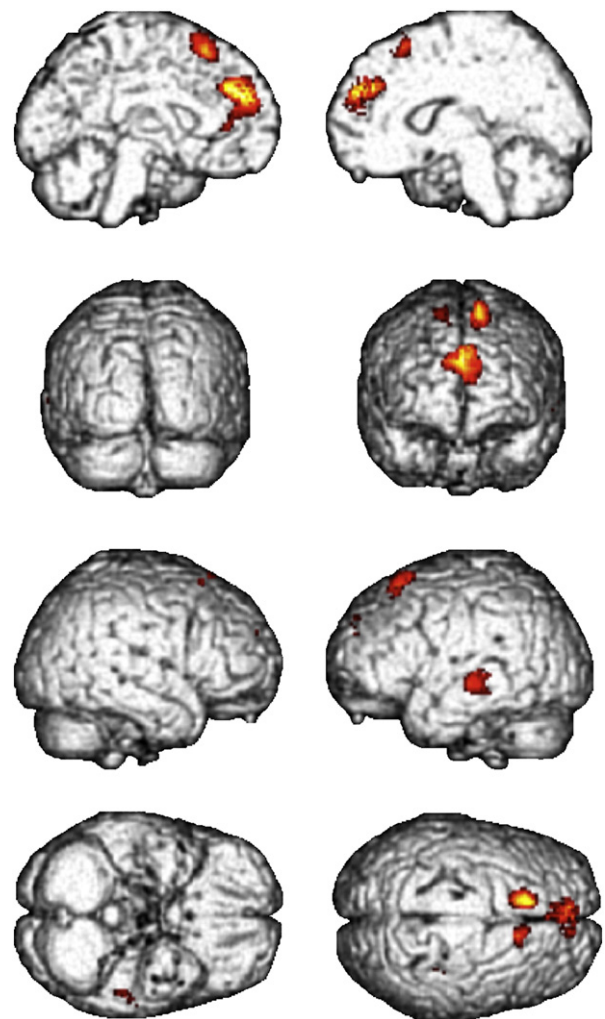
	Brodmann area	Hemi-sphere	Voxels	p Value	x	y	z
ROI-based analysis				Bonferroni			
HC > SZ							
Superior frontal gyrus	BA 6	L	325	0.000	−9	27	62
Superior frontal gyrus	BA 6	R	106	0.000	13	21	59
Medial frontal Gyrus	BA 9	bilateral	976	0.001	5	47	30
Superior temporal sulcus	BA 21/22	L	221	0.016	−53	−28	−4
ACC	BA 32	L	53	0.005	−16	40	11
Middle frontal gyrus	BA 8	L	60	0.002	−28	16	34
SZ > HC							
Gyrus rectus	BA 11	Bilateral	287	0.001	−9	35	−17
Frontal polar cortex	BA 10	Bilateral	166	0.038	−4	72	−4
Inferior frontal gyrus	BA 47	L	51	0.017	−30	32	−8
Inferior frontal gyrus	BA 47	R	68	0.010	34	36	−8
Inferior temporal gyrus	BA 20	L	34	0.024	−62	−22	−28
Inferior temporal gyrus	BA 20	R	49	0.000	42	−14	−28
Amygdala		R	38	0.008	14	−10	−24
Voxel-wise analysis				FDR			
HC > SZ							
Superior frontal gyrus	BA 6	L	325	0.000	−9	27	62
Medial frontal gyrus	BA 9	Bilateral	976	0.000	5	47	30
Superior temporal sulcus	BA 21/22	L	221	0.029	−53	−28	−4
SZ > HC							
Gyrus rectus	BA 11	Bilateral	287	0.001	−9	35	−17
Frontal polar cortex	BA 10	Bilateral	166	0.010	−4	72	−4

Fig. 2. Voxel-wise comparison of DMN maps contrasting healthy control subjects vs. schizophrenia patients at a threshold of p<0.005 uncorrected.

healthy controls, and found no significant correlation with total SANS scores in patients. We then performed an additional analysis of correlations with the five SANS subscales. Applying a threshold of p<0.05 (FDR corrected), we found significant negative correlations between the frontal polar cortex DMN activity and SANS subscales "affective flattening or blunting" ($\rho = 52$) and "alogia" ($\rho = 463$), as well as a negative correlation between the right inferior temporal gyrus and the "alogia" subscale ($\rho = 546$). There was no significant correlation between SANS scores and DMN areas with lower effects/connectivity in patients.

4. Discussion

In this study we assessed the default mode network (DMN) at rest in remitted patients with schizophrenia and healthy controls using a completely automated algorithm for extraction of the DMN component. Our findings can be summarised as revealing regional differences in the strength of effects, a relation to clinical symptoms, but no general breakdown in the overall anatomical composition of the network in schizophrenia.

Preceding our main analyses, the group comparison of goodness-of-fit indicates consistent detection of the DMN both in patients and controls without significant group differences. It therefore suggests that there is no systematic group difference in extracting the DMN and it also is an indicator of preserved overall architecture of the DMN in schizophrenia. This is contrary to other neuropsychiatric disorders such as Alzheimer's disease, where resting state analyses have goodness of fit for DMN analyses to actually distinguish patients from controls (Greicius et al., 2004). One previous report using ICA to

compare schizophrenia patients and healthy controls did find a stronger correlation of the healthy subjects' network with their default mode network template (Garrity et al., 2007). Comparing our findings to other studies, however, one should note that many other DMN studies have used functional MRI series from cognitive experiments (rather than resting-state data); so far, it is not clear whether DMN extraction and/or further analysis might be affected by this methodological difference and how spontaneous fluctuations might interact with amplitude changes caused by specific cognitive demands of a task. Of course, it is unclear whether such effects might be detected in larger sample sizes.

Our main analysis, on the other hand, provides evidence of differences in the regional contribution or strength of connectivity between groups, and hence DMN activity itself. Three findings are of particular interest. Firstly, we find several differences in prefrontal cortices, areas that have repeatedly been associated with schizophrenia pathology and its resulting cognitive impairments (Minzenberg et al., 2009). It is of interest to note that these differences include opposite effects for two sub-components of the DMN: while healthy controls show higher effects in dorsal prefrontal and temporal areas, patients show higher effects in some ventral areas of the prefrontal cortex, including the orbitofrontal cortex. This is an interesting pattern as it segregates different dysfunctions in schizophrenia: those associated with superior and middle frontal gyrus pathology (mostly cognitive), and those of the orbitofrontal cortex, often linked to affective flattening, impulsivity, and other clinical features of the disorder
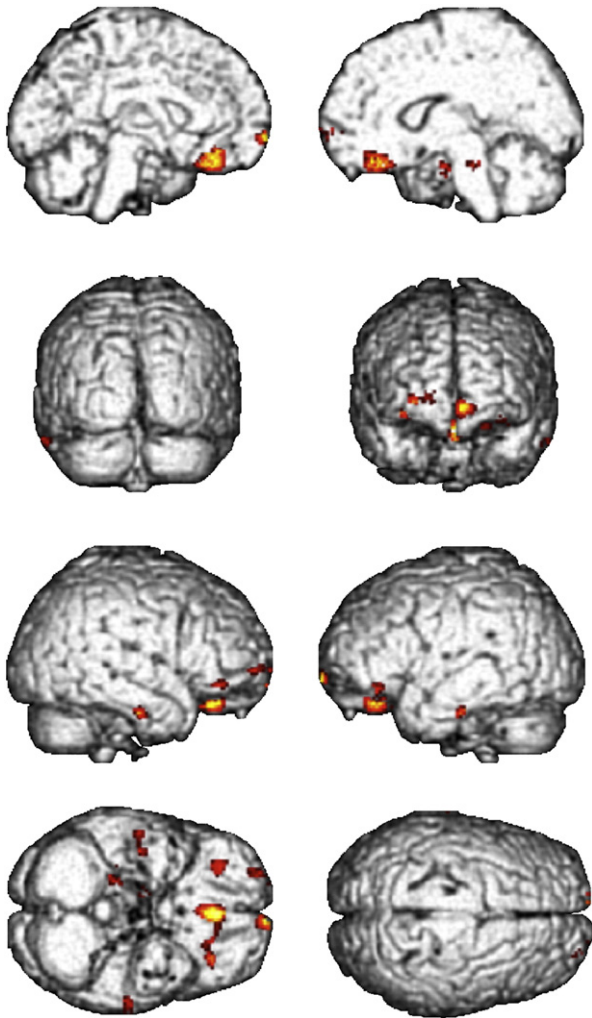
Fig. 3. Voxel-wise comparison of DMN maps contrasting schizophrenia patients vs. healthy control subjects at a threshold of p<0.005 uncorrected.

(Bellani et al., 2010). A similar spatial pattern of "hyperconnectivity" in orbitofrontal areas in patients (also extending to anterior frontopolar areas) has recently been identified with another methodological approach (Salvador et al., 2010). Given that some of these ventral areas, including the frontopolar node are correlated with negative psychopathology in our sample, this lends further support to the notion that this part of the DMN shows aberrant connectivity in schizophrenia and is relevant to its core pathophysiology. In contrast, our dorsal and medial prefrontal frontal findings corroborate findings from previous studies, which have also linked these abnormalities to cognitive deficits (Zhou et al., 2007; Huang et al., 2009; Kim et al., 2009), although with different methodologies. In this framework of a ventral–dorsal dissociation of effects, single nodes might be involved in different aspects related to either cognitive deficits or clinical symptoms (Kim et al., 2009). Secondly, we find a significant difference with patients showing higher effects in the amygdala. Dysfunction of this brain area has often been linked to both positive and negative symptoms in schizophrenia, including effects on emotional pathology (Aleman and Kahn, 2005). While we find higher effects in DMN connectivity, it is interesting to note that several fMRI studies using emotional and/or cognitive tasks have reported diminished amygdala activation in schizophrenia. For example, a recent study investigating amygdala reactivity to negative facial stimuli revealed a dissociation of activation difference related to the emotional task (Rasetti et al., 2009). This effect appears to be related to clinical state rather than genetic risk. Although our method does not provide

a direct assessment of baseline amygdala functioning (as measured by perfusion or metabolic scanning), but rather yields a measure of connectivity derived from pICA, it still appears conceivable that an increased baseline activity might explain the diminished effect during activation (i.e. smaller difference between baseline and activation state). This interpretation is also consistent with previous PET studies detecting elevated amygdala baseline activity in schizophrenia (Taylor et al., 2005). Post-hoc testing revealed that the amygdala effect was also present in the left amygdala, but failed to reach statistical significance. Thirdly, it is interesting to note that our correlations with psychopathology are restricted to those areas where patients show higher DMN connectivity effects, especially in the ventral areas of the frontal pole. As discussed above, this might be related to the fact that the group differences in the dorsal frontal areas are rather related to cognitive deficits of the disorder rather than (negative) symptoms.

Finally, we need to consider a few limitations of the study. Although our automated algorithm for extraction of the DMN component relies on well-established findings of previous studies (Shulman et al., 1997), thus making it susceptible to refinement of the DMN anatomical definition, this definition served well to reliably extract the DMN component in all subjects. Also, our voxel-wise analysis of all subjects included allows consideration of the potential variability of the DMN in this cohort studied. Secondly, we need to consider the fact that patients were on antipsychotic medication, suspension of which would not have been justified on ethical grounds. A recent study reported effects of olanzapine on resting state activity (Sambataro et al., 2010), however, data were acquired during a cognitive fMRI experiment (rather than resting state).

In conclusion, our study demonstrates the successful use of a fully automated algorithm for the detection and reliable extraction of DMN activity from resting-state fMRI data in schizophrenia. Our findings suggest that schizophrenia is associated with regional difference (both hyper- and hypoconnectivity) of single nodes of the default mode network, which appear to be related to specific core symptoms of the disorder.

Supplementary materials related to this article can be found online at doi:10.1016/j.schres.2012.01.036.

Contributors

I.N., G.M., C.G., and H.S. designed the study.

I.N., St.S., and H.S., contributed to patient recruitment and scanning.

I.N., K.L., M.D., H.P.B., C.G., J.R.R., R.G.M.S., and H.S. contributed to the data collection, processing, and pre-processing.

G.M., G.W., C.G., R.M., and I.N. contributed to implementation of the image processing pipeline and imaging data analysis.

G.M. and I.N. wrote the first drafts of the manuscript and all authors commented on and approved the final version.

References

Aleman, A., Kahn, R.S., 2005. Strange feelings: do amygdala abnormalities dysregulate the emotional brain in schizophrenia? Prog. Neurobiol. 77, 283–298.
Auer, D.P., 2008. Spontaneous low-frequency blood oxygenation level-dependent fluctuations and functional connectivity analysis of the 'resting' brain. Magn. Reson. Imaging 26, 1055–1064.

Beckmann, C.F., Smith, S.M., 2004. Probabilistic independent component analysis for functional magnetic resonance imaging. IEEE Trans. Med. Imaging 23, 137–152.

Beckmann, C.F., Smith, S.M., 2005. Tensorial extensions of independent component analysis for multisubject FMRI analysis. NeuroImage 25, 294–311.

Beckmann, C.F., DeLuca, M., Devlin, J.T., Smith, S.M., 2005. Investigations into resting-state connectivity using independent component analysis. Philos. Trans. R Soc. Lond. B Biol. Sci. 360, 1001–1013.

Bellani, M., Cerruti, S., Brambilla, P., 2010. Orbitofrontal cortex abnormalities in schizophrenia. Epidemiol. Psichiatr. Soc. 19, 23–25.

Bluhm, R.L., Miller, J., Lanius, R.A., Osuch, E.A., Boksman, K., Neufeld, R.W., Theberge, J., Schaefer, B., Williamson, P., 2007. Spontaneous low-frequency fluctuations in the BOLD signal in schizophrenic patients: anomalies in the default network. Schizophr. Bull. 33, 1004–1012.

Broyd, S.J., Demanuele, C., Debener, S., Helps, S.K., James, C.J., Sonuga-Barke, E.J., 2009. Default-mode brain dysfunction in mental disorders: a systematic review. Neurosci. Biobehav. Rev. 33, 279–296.

Calhoun, V.D., Maciejewski, P.K., Pearlson, G.D., Kiehl, K.A., 2008. Temporal lobe and "default" hemodynamic brain modes discriminate between schizophrenia and bipolar disorder. Hum. Brain Mapp. 29, 1265–1275.

Damoiseaux, J.S., Rombouts, S.A., Barkhof, F., Scheltens, P., Stam, C.J., Smith, S.M., Beckmann, C.F., 2006. Consistent resting-state networks across healthy subjects. Proc. Natl. Acad. Sci. U. S. A. 103, 13848–13853.

Garrity, A.G., Pearlson, G.D., McKiernan, K., Lloyd, D., Kiehl, K.A., Calhoun, V.D., 2007. Aberrant "default mode" functional connectivity in schizophrenia. Am. J. Psychiatry 164, 450–457.

Greicius, M., 2008. Resting-state functional connectivity in neuropsychiatric disorders. Curr. Opin. Neurol. 21, 424–430.

Greicius, M.D., Srivastava, G., Reiss, A.L., Menon, V., 2004. Default-mode network activity distinguishes Alzheimer's disease from healthy aging: evidence from functional MRI. Proc. Natl. Acad. Sci. U. S. A. 101, 4637–4642.

Greicius, M.D., Flores, B.H., Menon, V., Glover, G.H., Solvason, H.B., Kenna, H., Reiss, A.L., Schatzberg, A.F., 2007. Resting-state functional connectivity in major depression: abnormally increased contributions from subgenual cingulate cortex and thalamus. Biol. Psychiatry 62, 429–437.

Greicius, M.D., Kiviniemi, V., Tervonen, O., Vainionpaa, V., Alahuhta, S., Reiss, A.L., Menon, V., 2008. Persistent default-mode network connectivity during light sedation. Hum. Brain Mapp. 29, 839–847.

Hoptman, M.J., Zuo, X.N., Butler, P.D., Javitt, D.C., D'Angelo, D., Mauro, C.J., Milham, M.P., 2010. Amplitude of low-frequency oscillations in schizophrenia: a resting state fMRI study. Schizophr. Res. 117, 13–20.

Huang, X.Q., Lui, S., Deng, W., Chan, R.C., Wu, Q.Z., Jiang, L.J., Zhang, J.R., Jia, Z.Y., Li, X.L., Li, F., Chen, L., Li, T., Gong, Q.Y., 2009. Localization of cerebral functional deficits in treatment-naive, first-episode schizophrenia using resting-state fMRI. NeuroImage 49, 2901–2906.

Kim, D.I., Manoach, D.S., Mathalon, D.H., Turner, J.A., Mannell, M., Brown, G.G., Ford, J.M., Gollub, R.L., White, T., Wible, C., Belger, A., Bockholt, H.J., Clark, V.P., Lauriello, J., O'Leary, D., Mueller, B.A., Lim, K.O., Andreasen, N., Potkin, S.G., Calhoun, V.D., 2009. Dysregulation of working memory and default-mode networks in schizophrenia using independent component analysis, an fBIRN and MCIC study. Hum. Brain Mapp. 30, 3795–3811.

Mantini, D., Perrucci, M.G., Del Gratta, C., Romani, G.L., Corbetta, M., 2007. Electrophysiological signatures of resting state networks in the human brain. Proc. Natl. Acad. Sci. U. S. A. 104, 13170–13175.

McKeown, M.J., Jung, T.P., Makeig, S., Brown, G., Kindermann, S.S., Lee, T.W., Sejnowski, T.J., 1998. Spatially independent activity patterns in functional MRI data during the Stroop color-naming task. Proc. Natl. Acad. Sci. U. S. A. 95, 803–810.

Minzenberg, M.J., Laird, A.R., Thelen, S., Carter, C.S., Glahn, D.C., 2009. Meta-analysis of 41 functional neuroimaging studies of executive function in schizophrenia. Arch. Gen. Psychiatry 66, 811–822.

Oldfield, R.C., 1971. The assessment and analysis of handedness: the Edinburgh inventory. Neuropsychologia 9, 97–113.

Ongur, D., Lundy, M., Greenhouse, I., Shinn, A.K., Menon, V., Cohen, B.M., Renshaw, P.F., 2010. Default mode network abnormalities in bipolar disorder and schizophrenia. Psychiatry Res. 183, 59–68.

Raichle, M.E., Snyder, A.Z., 2007. A default mode of brain function: a brief history of an evolving idea. NeuroImage 37, 1083–1090 (discussion 1097–1089).

Raichle, M.E., MacLeod, A.M., Snyder, A.Z., Powers, W.J., Gusnard, D.A., Shulman, G.L., 2001. A default mode of brain function. Proc. Natl. Acad. Sci. U. S. A. 98, 676–682.

Rasetti, R., Mattay, V.S., Wiedholz, L.M., Kolachana, B.S., Hariri, A.R., Callicott, J.H., Meyer-Lindenberg, A., Weinberger, D.R., 2009. Evidence that altered amygdala activity in schizophrenia is related to clinical state and not genetic risk. Am. J. Psychiatry 166, 216–225.

Rotarska-Jagiela, A., van de Ven, V., Oertel-Knochel, V., Uhlhaas, P.J., Vogeley, K., Linden, D.E., 2010. Resting-state functional network correlates of psychotic symptoms in schizophrenia. Schizophr. Res. 117, 21–30.

Salvador, R., Sarro, S., Gomar, J.J., Ortiz-Gil, J., Vila, F., Capdevila, A., Bullmore, E., McKenna, P.J., Pomarol-Clotet, E., 2010. Overall brain connectivity maps show cortico-subcortical abnormalities in schizophrenia. Hum. Brain Mapp. 31, 2003–2014.

Sambataro, F., Blasi, G., Fazio, L., Caforio, G., Taurisano, P., Romano, R., Di Giorgio, A., Gelao, B., Lo Bianco, L., Papazacharias, A., Popolizio, T., Nardini, M., Bertolino, A., 2010. Treatment with olanzapine is associated with modulation of the default mode network in patients with schizophrenia. Neuropsychopharmacology 35, 904–912.

Shulman, G.L., Fiez, J.A., Corbetta, M., Buckner, R.L., Miezin, F.M., Raichle, M.E., Petersen, S.E., 1997. Common blood flow changes across visual tasks: II. Decreases in cerebral cortex. J. Cogn. Neurosci. 9, 648–663.

Taylor, S.F., Phan, K.L., Britton, J.C., Liberzon, I., 2005. Neural response to emotional salience in schizophrenia. Neuropsychopharmacology 30, 984–995.

van den Heuvel, M.P., Hulshoff Pol, H.E., 2010. Exploring the brain network: a review on resting-state fMRI functional connectivity. Eur. Neuropsychopharmacol. 20, 519–534.

Whitfield-Gabrieli, S., Thermenos, H.W., Milanovic, S., Tsuang, M.T., Faraone, S.V., McCarley, R.W., Shenton, M.E., Green, A.I., Nieto-Castanon, A., LaViolette, P., Wojcik, J., Gabrieli, J.D., Seidman, L.J., 2009. Hyperactivity and hyperconnectivity of the default network in schizophrenia and in first-degree relatives of persons with schizophrenia. Proc. Natl. Acad. Sci. U. S. A. 106, 1279–1284.

Woodward, N.D., Rogers, B., Heckers, S., 2011. Functional resting-state networks are differentially affected in schizophrenia. Schizophr. Res. 130, 86–93.

Zhou, Y., Liang, M., Tian, L., Wang, K., Hao, Y., Liu, H., Liu, Z., Jiang, T., 2007. Functional disintegration in paranoid schizophrenia using resting-state fMRI. Schizophr. Res. 97, 194–205.